Scientific Research Publishing

Advances in Microbiology, 2018, 8, *-*
http://www.scirp.org/journal/aim
ISSN Online: 2165-3410
ISSN Print: 2165-3402

E-coli Accumulation behind an Obstacle

Gastón L. Miño[1*], Magali Baabour[2], Ricardo Chertcoff[2], Gabriel Gutkind[3], Eric Clément[4], Harold Auradou[5], Irene Ippolito[2]

[1]Lab. de Microscopía Aplicada a Estudios Moleculares y Celulares (LAMAE), Fac. de Ingeniería, Univ. Nac. de Entre Ríos (FI-UNER) and Inst. de Investigación y Desarrollo en Bioingeniería y Bioinformática IBB-(UNER-CONICET), Oro Verde, Argentina
[2]Universidad de Buenos Aires,Facultad de Ingeniería, Grupo de Medios Porosos, Buenos Aires, Argentina
[3]Universidad de Buenos Aires, Facultad de Farmacia y Bioquímica, Cátedra de Microbiología, Buenos Aires, Argentina
[4]Physique et Mécanique des Milieux Hétérogénes (UMR 7636 ESPCI/CNRS/Univ. P.M. Curie/Univ. Paris-Diderot), Paris, France
[5]Laboratoire FAST, Univ. Paris Sud, CNRS, Université Paris-Saclay, F-91405 Orsay, France
Email: *glmino@ingenieria.uner.edu.ar

How to cite this paper: Author 1, Author 2 and Author 3 (2018) Paper Title. *Advances in Microbiology*, **8**, *-*.
https://doi.org/10.4236/***.2018.*****

Received: **** **, ***
Accepted: **** **, ***
Published: **** **, ***

Abstract

This paper describes our findings regarding the accumulation of motile bacteria at the rear of a confined obstacle and the physical description of the mechanisms at play. We found that the modification of flow due to the presence of the obstacle produces vorticity that favor the diffusion of bacteria towards the downstream stagnation point. By testing different flow rates, we determined the range in which bacteria accumulate. More interestingly, we observe that hydrodynamic interaction between the bacteria and the top and bottom surface of the microfluidic chip maintain the bacteria in the region where the flow velocity is lower than their own velocity. In the case of non-motile bacteria, this effect is not observed because bacteria follow the streamlines as passive tracers do.

Keywords

E-coli, Motility, Filtration, Microfluidic, Bacterial Accumulation

1. Introduction

Particles fixation is the process that enables to purify, decontaminate and clean waste water. It is also one of the processes used to number microorganisms contained in fluids. In practice, the removal of bacteria or colloids is achieved by flowing the fluid through filters. Different types of filters exist: Membranous filters filter bacteria on the surface whereas porous filters are a depth filtration system. In water waste treatment, biofilters and slow sand filters fall in the latter

classification, and contaminants, particles and microorganisms are retained while water flows slowly through the pores [1] [2] [3]. Slow sand filters work through the formation of a biofilm in the top few millimeters of the fine sand layer. The initial step of the formation of the filtration layer is triggered by the fixation of bacteria on the grains [4]. Biomass grows from these spots and the surface biofilm provides an effective purification in water treatment. Different factors are known to influence the adhesion of the bacteria and the formation of the biofilm [4] [5]. Physico-chemical factors like the grain sizes, possible presence of organic matter, water flow velocity, ionic strength, pH but also bacterial properties including size, shape and surface are known to influence the adhesion.

Very few studies questioned the influence of bacteria motility on adhesion. And mainly because it is difficult—if not impossible—to impose all the necessary experimental conditions. In consequence, the exact influence of motility on the adhesion is poorly understood. In a recent study, Nelson and coworkers addressed this point using numerical modelling. They assumed that the trajectory of bacteria is a random succession of "runs" and "tumbles". The aim of their study was to determine the influence of motility on the transport to the grain surface. Unfortunately, they fail to measure any difference between motile and non-motile bacteria repartition on the surface of the grains.

Thanks to the recent development of microfluidic, researchers were able to visualize and track trajectories of bacteria in "simple" flow geometries [6] [7] [8] [9] [10]. For instance, some of us have investigated the influence of a constriction in a rectangular channel and found that the interplay between upstream swimming at the edges [10] and erosion at the constriction produces strong bacteria accumulation passing the constriction which pertains over large distances along the flow. These studies revealed non-trivial influences of the flow on the bacteria trajectories. These effects are ignored in the model of Nelson and coworkers that assumed bacteria were passive particles in the flow.

In the present work, we study the transport of motile and non motile bacteria under flow using a microfluidic device with a circular obstacle that mimics a grain. This enables us to carry out the experience previously done by model by Nelson and coworkers [11].

We observe under a wide range of flow velocity an over-concentration of bacteria downstream the obstacle. This over-concentration is not present with non-motile bacteria. We thus prove that motility does indeed influence the transport of motile bacteria around the grain and favor the presence of bacteria in the region of low velocity (*i.e.* at the rear of grain). Finally, we give the basic physical ingredients that lead to the accumulation.

2. Materials and Methods

2.1. Preparation and Characterization of the Bacterial Suspension

We use wild type Escherichia coli W, ATCC 11105 [12]. The culture is first

grown overnight in Luria Broth (LB) medium (40 µl of this solution is then diluted in 10 ml of LB) at 37˚C. This suspension is placed in a shaker (at 37˚C and 200 rpm) for at least 5 hr in order to reach the maximal activity [13]. Cells are centrifuged (1000 × g for 10 min) and resuspended in Minimal Motility Media (MMA) to minimize cell division and favor swimming. MMA consists in 10 mM NaH_2PO_4, 10 mM K_2HPO_4, 0.1 mM EDTA, and 20 mM Sodium Lactate, supplemented with K-acetate (0.34 mM) [14].

Experiments are performed at room temperature T = 25˚C with suspensions (MMA solution + bacteria) containing (1 ± 0.2) 10^8 bacteria/ml. This concentration is low enough so that no large scale collective motion is visible. Suspensions of non-motile bacteria or "dead" bacteria were obtained by adding 1 µg/ml of formaldehyde to the suspension. Since the microfluidic channel is made in PDMS, oxygen can pass through the polymeric structure. The bacteria concentration is such that no stress due to the lack of oxygen is created. In these conditions the bacteria perform a run and tumble motion, characterized by a mean velocity v_b = 25 ± 9 µm/s and an active diffusivity D = 131 ± 56 µm^2/s calculated for trajectories longer than 1 s.

In order to compute v_b the velocity distribution was obtained considering 2450 trajectories of bacteria swimming within the channel far away from the obstacle at zero flow. D was obtained computing the Mean Square Displacement (MSD) for all the trajectories.

2.2. Microfluidic Device Preparation and Flow Visualization

A microfluidic channel of total length L = 15 mm, height h = 20 µm, width W = 200 µm with one cylindrical obstacle of radius R = 80 µm was made of PDMS (see **Figure 1**) and glued to a glass microscope slide using plasma bounding. **Figure 1** shows a sketch of the channel and a picture of the obstacle portion of the channel. The inlet of the channel is connected to the bacterial suspension reservoir and the outlet to a waste reservoir. The flow within the channel is achieved by gravity overpressure by varying the height between the reservoir and

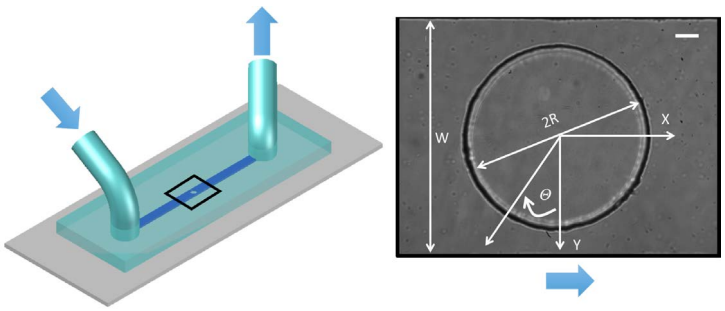

(a) (b)

Figure 1. (a) Schematic representation of the chip: height (h = 20 µm), width (W = 200 µm) and length (L = 15 mm); (b) Snapshot of the central part of the channel showing the obstacle of radius R = 80 µm. Arrow shows the direction of the flow. The angle Θ is defined in such way that the front and the rear of the obstacle coincide with 90˚ and 270˚, respectively. Top-left bar = 20 µm.

the waste. The direction of the flow defines the up and downstream stagnation point and the angle definition in **Figure 1(b)**.

The Reynolds number Re = ρU h/η, with ρ and η are respectively the density and dynamic viscosity of the MMA, and U the mean fluid velocity is of the order of 10^{-3}, giving a laminar flow with no presence of vortices. We work essentially in confined conditions meaning that the vertical channel height h is such that the typical time for a bacterium to cross the channel is shorter or comparable to the persistence time. Bacteria are imaged by a phase-contrast technique using an inverted microscope with 40X magnification dry objective.

Images were recorded with a digital camera PixeLINK PL-A741-E and the visualization field is 740 × 1000 pixels^2 giving an area of 200 × 270 μm^2. Videos are captured at a frame rate of 30 frame per second for 10s. Due to the small height of the channel, bacteria swimming on the bottom and top walls are imaged simultaneously. For every image sequence, an image containing the median value of each pixel is created and subtracted to each image of the sequence. This operation removes dust on lens surfaces or stuck bacteria which can possibly hinder the tracking. Once the images are processed, a Fiji plugin called Trackmate [15] is used to identify motile bacteria and track their trajectories (See Supplementary_Movie_SM1.avi and Supplementary_Movie_SM1_Tracks.avi). Tracking consists of two main processes; first by detecting the spots in a series of frames (segmentation process) and subsequently linking them over these frames to build the tracks (tracking process).

Movies are also taken up and downstream at a distance from the obstacle. They are used to determine the mean flow velocities U.

2.3. Flow Field Close to the Obstacle

The microfluidic device used for the experiments is a rectangular section channel with a cylindrical obstacle placed in the middle of the channel (see **Figure 1**). Finite element method (FEM) on COMSOL Multiphysics Software 5.0 (Comsol Inc., MA) was used to solve the Navier-Stokes equations in the same geometry. A constant pressure difference ΔP is imposed between the inlet and outlet surfaces. After the determination of the velocity $v(x, y, z)$ on each node, we computed the average flow velocity in the gap by numerical integration of the magnitude of v over the height of the channel such that

$$v(x.y) = \frac{1}{h}\int_0^h v(x, y, z)\, dz \quad .$$

Same criteria were used to compute the average shear rate over height.

3. Results

3.1. Qualitative Observation of the Density of Bacteria in the Vicinity of the Obstacle

The **Figure 2** shows the overlay of all the images obtained in 10 s experiments

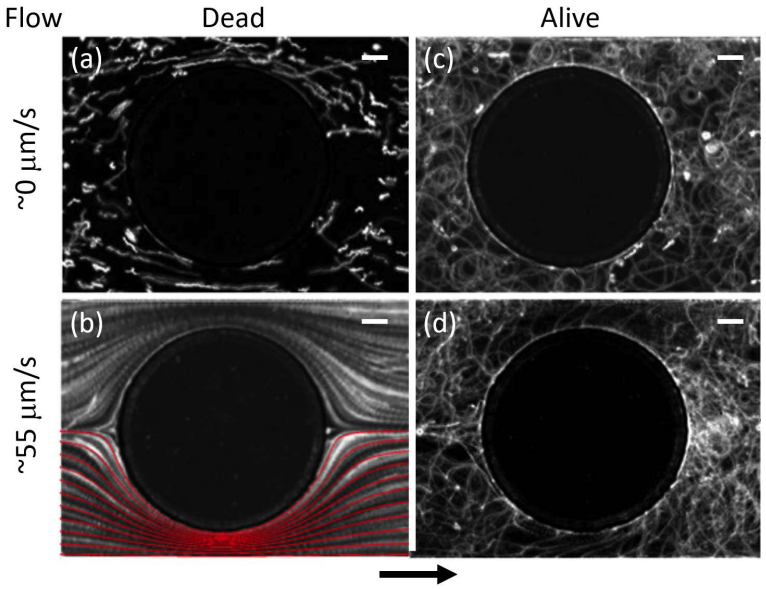

Figure 2. (a) Superpositions of images recorded during 10s experiments performed with non-motile (first column) or motile (second column) bacteria at different flow velocities around the obstacle (black region in the center of the image). In the first row, the average flow velocity is ~0 µm/s while in the second row, U = 55 µm/s. Red lines show the streamlines obtained by numerical simulation. Top-left bars = 20 µm.

using either non-motile or motile bacteria for two flow conditions: i) zero and ii) the onset flow that produces accumulation.

In a quiescent fluid (**Figure 2(a)**), non-motile bacteria experience a random Brownian motion with a slight translational motion indicating the existence of a small residual background flow of the order of 1 µm/s. In the presence of a flow (**Figure 2(b)**) the traces left by the trajectories of the dead bacteria (white lines in **Figure 2(b)**) overlay evidently with the streamlines (in red) obtained by numerical simulation.

In the case of living bacteria and at zero flow, bacteria move mostly along circular trajectories and few of them make quasi-straight paths. These circular trajectories result from the hydrodynamic interaction between the auto-propelled organisms and the surface [16] [17] [18]. Moreover, they are observed to occupy the entire channel homogeneously (**Figure 2(c)**).

When a flow is imposed, the motile bacteria are not observed to follow the streamlines. Instead, we observe the appearance of a lightened area at the rear of the obstacle identifying a clear accumulation of the bacteria in that particular region (**Figure 2(d)** and Supplementary_Movie_SM1.avi).

3.2. Influence of the Flow on the Accumulation

To quantify this accumulation effect over the range of flows, we compute the number of bacteria detected per pixel and per unit of time in each image sequence. We then consider an annular portion thickness of 10 µm surrounding the obstacle. This annular section is then divided in 36 sections of equal size. The

average number of bacteria in each section N_Θ is finally calculated. The **Figure 3(a)** and **Figure 3(c)** show, this number N_Θ normalized by the average number of bacteria detected far from the obstacle N for two extreme flow values; this is when the effect starts to show and when it disappears. Under flow, the lateral sides of the obstacle ($\Theta = 0$ and 180˚, see **Figure 1(b)** for the definition of Θ) are clearly depleted and almost no bacteria are detected in those sections. We also see a clear downstream accumulation demonstrated by a net increase in the number of detected bacteria well above the value detected far from the obstacle.

We next extract, for all flow values, the maximum value of the normalized concentration P_- and P_+ at the stagnation points located upstream ($\Theta = 90˚$) and downstream ($\Theta = 270˚$), respectively. We see that the number of positions detected is always higher downstream. The number P_- measured up-stream is constant and close to 1 (see **Figure 3(b)**), *i.e.* similar bacterial concentration as in the rectangular part far away from the obstacle. Interestingly, the values of P_+ suggest the bacteria stay longer resulting in a doubled accumulation.

Next we compute the standard deviation σ_- and σ_+ of the normalized concentration distribution around the upstream and downstream peaks P_- and P_+,

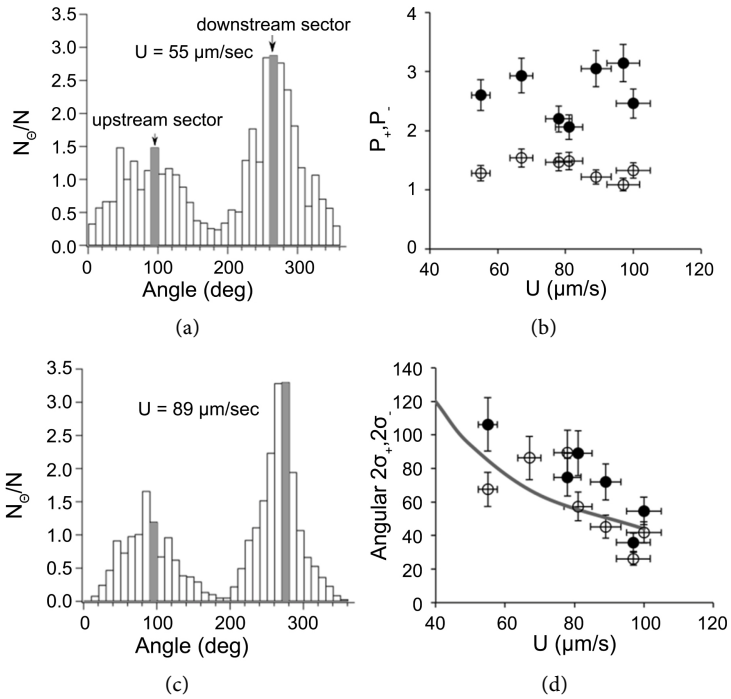

Figure 3. (a) and (c) Distribution of the average number of bacteria detected by unit of time around the obstacle for two flow velocities U = 55 and 89 µm/s. The average is done in an annulus of width 10 µm around the obstacle and cut in 36 sectors of 10 degrees. The measurements are finally normalized by the average number of bacteria detected by unit of time away from the obstacles; (b) and (d) Variation of the maximum value of the normalized number of positions detected P and the standard deviation σ as function of U. Filled symbols show the values measured downstream (*i.e.* in the sector $\Theta = 270 \pm 10˚$). Empty symbols are for the values measured upstream (*i.e.* for $\Theta = 90 \pm 10˚$). The solid curve shows the width of regions lining the obstacle where the flow velocity is lower than v_b.

respectively. We observe that this quantity narrows when the flow increases (see **Figure 3(d)**). This means that the area where bacteria accumulate shrinks when the flow increases. When we define an angular region where the fluid velocity is lower than bacterial mean swimming speed v_b (see gray curve in **Figure 3(d)** and Material and Methods section), we observe the same behavior.

The difference between motile and non-motile is also highlighted by studying the distribution of velocity component v_x along the flow (See **Figure 4(a)**). First, let us consider non-motile bacteria flowing at 40 μm/s. We notice that the distribution reflects the their convective behavior (diamond curve at **Figure 4(a)**). Then we consider the distribution of motile bacteria under zero flow (square curve at **Figure 4(a)**) and notice that their distribution is dependent on their own mobility as it has been classically observed [19] [20]. Finally, when a flow is imposed, the velocity distribution of motile bacteria (circle curve **Figure 4(a)**) is the combination of the two distributions: the one that dependent of the convective behavior and the one that depends on their own motility with a clear peak at v_x =0 μm/s.

In order to separate these two behaviors, we apply a threshold of $v_x = v_b$ on the velocities to separate the trajectories of the bacteria into two families (see **Figure 4(a)** and **Figure 4 (c)**). In the $v_x < v_b$ family (**Figure 4(b)**) we see a clear accumulation of the trajectories at the front and more importantly at the rear of the obstacle. In the $v_x > v_b$ family, this accumulation is not observed (**Figure 4(c)**) and we recognize the pattern visualized in **Figure 2(b)**.

3.3. Flow Field Close to the Obstacle and its Effect on the Accumulation

In **Figure 5(a)**, we can see the lines separating regions where the magnitude of

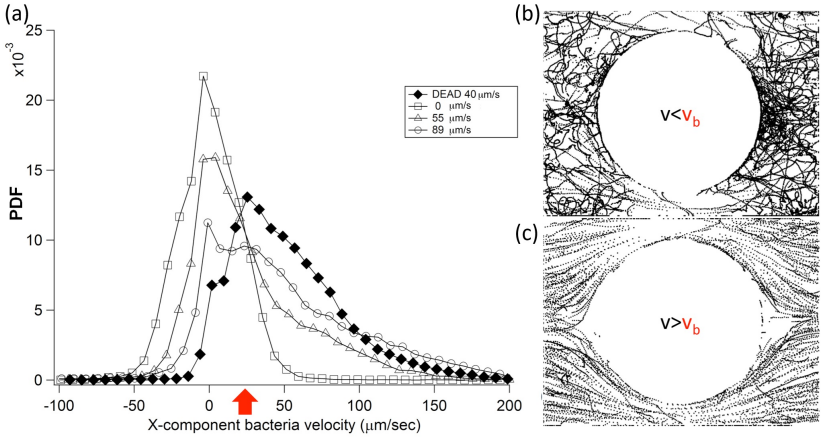

Figure 4. (a) Probability Function Distributions (PDF) of the velocity component v_x of motile bacteria flowing at U = 0 (squares), 55 (triangles) and 89 μm/s (circles). Black diamonds represent non-motile bacteria imposing a flow velocity of U = 40 μm/s. The distributions are vertically rescaled for convenience; (b) Trajectories along which motile bacteria have a velocity below v_b; (c) Trajectories having a velocity higher than v_b. The red arrow indicates the magnitude of the average swimming velocity $|v_b|$ = 25 μm/s. Top-left bars = 20 μm.

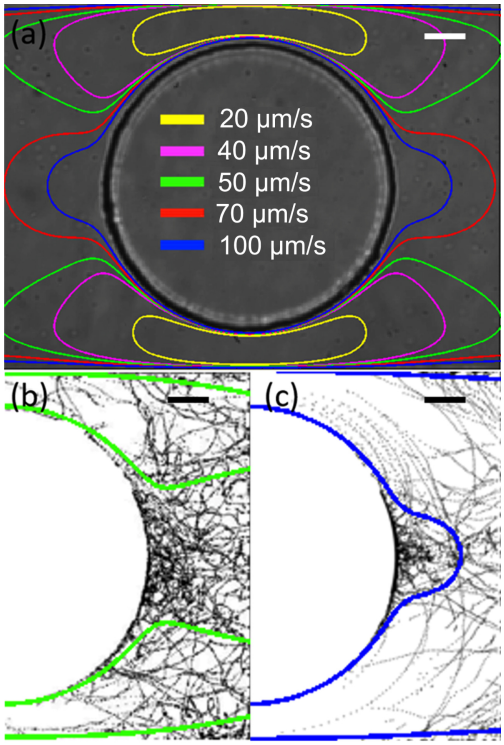

Figure 5. (a) Microchannel snapshot with superposition of isovelocity curves obtained from the simulation at different flow U (yellow, U = 20 μm/s; magenta, U = 40 μm/s; green, U = 50 μm/s; red, U = 70 μm/s; and blue, U = 100μm/s). Each color represents the isovelocity corresponding to 25 μm/s. Snapshot of the trajectories with a velocity lower than v_b with superposition of the isovelocity of v = 25 μm/s for a flow velocity (b) U = 55 μm/s and (c) U = 89 μm/s. The areas show in (b) and (c) are those of maximal bacterial accumulation (*i.e.* the downstream side). Top-left bars = 20 μm.

the fluid velocity is higher than the swimming velocity v_b from the region where the fluid velocity is lower than v_b for different imposed flows U. For flows lower that U = 57 μm/s, the areas with flow velocities larger than v_b are found in lobes at both sides of the obstacle (between the lateral wall and the obstacle), this means that the entire channel before and after the obstacle has mean flow velocities lower than v_b and bacteria are swimming outside those lateral areas. The situation changes when the flow is higher than U = 57 μm/s. In this case, the region with low velocity shifts to the front and rear of the obstacles and to two narrow lateral wall zones. These regions diminish as the flow is increased. As consequence the areas with velocities lower than v_b get narrowed with the flow (see gray curve in **Figure 3(d)**).

If we now superimpose to the trajectories with a velocity smaller than v_b (applying the same threshold as in **Figure 4(b)** and **Figure 4 (c)**), we observe that bacteria dwell in areas with low velocity. **Figure 5(b)** and **Figure 4 (c)** exemplify two cases with different mean flow: the onset and the maximal flow where the accumulation phenomenon is observed. In the first case, bacteria can occupy the entire channel except for those regions inside of the lateral lobes. In the second, bacteria accumulate in the rear of the obstacle. This reveals that the bacteria ac-

cumulate in the region where the flow velocity is lower than the swimming velocity.

4. Physical Description of the Accumulation Phenomenon

In order to understand the accumulation we have highlighted three steps (See **Figure 6**): 1) the flow of the bacteria towards the rear of the obstacle, 2) their trapping, and 3) the replenishment of the trapping zone.

1) the flow to the rear of the obstacle

To explain this phenomenon, we assume that bacteria (body + flagella) can be modelled by a rod moving at a constant swimming velocity v_b along its principal axis. We also consider that the flow and the motility of the bacteria are in the plane (x, y).

In a shear, because of their elongated shape, rods spin at an average rotational velocity equal to the local vorticity of the flow [21]. During each rotation due to their swimming abilities and the random change in the swimming direction, rods cross streamlines and explore the (x, y). In the presence of a gradient of vorticity, this results in a net flux of rods from the low to the high vorticity region [9].

In our geometry and in the plane (x, y), the vorticity comes from the flow in the constriction between the obstacle and the walls. In this section, the vorticity is maximal on the surfaces, decreases to zero as the distance from the surfaces increases. There is thus a flux of bacteria directed from the thick dotted line in **Figure 6** to the surfaces. As a consequence, bacteria located between this line and the obstacle will diffuse toward the obstacle.

2) trapping mechanism

Meanwhile the bacteria move toward the obstacle, they are convected with the

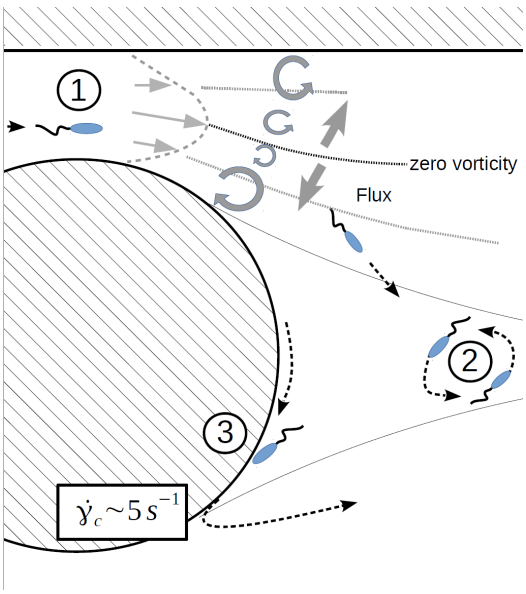

Figure 6. Tentative scenario for the accumulation: 1) the flow of the bacteria towards the rear of the obstacle, 2) the trapping, and 3) the replenishment of the trapping zone.

flow with decreasing velocity. Once they arrive in a region where the magnitude of the fluid velocity is lower than the swimming velocity, the hydrodynamic interaction between the bacteria and the top and bottom surfaces of the microfluidic chip comes into play [22] [16]. Because of this interaction, bacteria swim in clockwise, circular trajectories near the surfaces (as indeed show in **Figure 4(b)** and **Figure 5**). The interaction is known to be responsible for the accumulation of bacteria on the surface [17] [23]. Some of the bacteria are observed to flow to the obstacle. Once they reach the surface, they are found to swim along the surface of the obstacle [6].

3) the replenishment of the trapping zone

While swimming along the obstacles, the bacteria face a flow of increasing strength making their upstream motion harder and harder. Previous studies have revealed that *E-coli* bacteria can move upstream as long as the shear rate is below 5 s^{-1}. For low flows, the simulation reveals that the shear around the surface of the obstacle is mainly below this threshold (see supplementary **Figure S1**). Experimentally, for flows U lower than 55 μm/s, bacteria accumulate on the surface and turn around the obstacle. It is only because of the random change of swimming direction that the bacteria eventually leave the surface. Above U = 55 μm/s, the shear rate reaches 5 s^{-1} downstream of the constriction (This situation is depicted in **Figure 6**). In this case, while moving along the surface, bacteria faces a flow so strong that it pulls the bacteria away from the surface bringing them back in the flow. Some of them come back to the rear of the obstacle thanks to 1).The simulation shows that the areas around the surface obstacle with shear lower than 5 s^{-1} decrease when the flow increases (see supplementary **Figure S1**).

The net effect of 1), 2) and 3) is an accumulation at the rear of the obstacle for U>55 μm/s. Increasing U increases the vorticity gradient in the plan (*x*, *y*) and thus increases 1). But the region where the velocity is lower than the swimming velocity decreases reducing the area in which the bacteria accumulate.

5. Discussion and Conclusion

Bacterial trapping in biofilter and slow sand filter involves both physical and biological processes [2]. The classical physico-chemical view of filtration does not take into account microorganism motility nor their hydrodynamic interactions with walls. In the absence of flow, bacteria can be hydrodynamically "trapped" on solid surfaces and the range of this effect is within 10 microns from them [17]. Around spheres or cylindrical obstacles this effect is also observed [24] [25]. Moreover, reducing the cylinder diameter reduces the capture capacity. Increasing the radius increases the hydrodynamic interaction leading to bacterial accumulation around the obstacle [23]. In the presence of flow, the scenario changes and different mechanisms modify the transport of bacteria and their accumulation around the obstacle.

In our experiments, we explore the transport and accumulation of bacteria

around an obstacle with a grain size that allows accumulation along surfaces and we study the effect of the flowing fluid on the accumulation areas.

We identify vorticity gradient as a major effect enabling the drift of bacteria towards low velocity region. In our experiments, the vorticity gradient is due to the obstacle filling almost entirely the width of the channel leaving only constriction space of similar size to the chip aperture. Furthermore, the hydrodynamic interactions of motile bacteria and surfaces are sufficiently strong to trap bacteria. In future research, by modifying the shape and curvature of the obstacle we expect to enhance the bacterial trapping capacity.

Our findings give some important insights on the role of the motility leading to the accumulation and attachment of bacteria in a natural environment. By identifying the physical mechanisms at play, it may also guide future researches aiming to develop techniques to filter and separate motile microorganism in microbiology.

Acknowledgements

This work is supported by a public grant from the "Laboratoired' Excellence Physics Atom Light Mater" (LabEx PALM) overseen by the French National Research Agency (ANR) as part of the "Investissementsd' Avenir" program (reference: ANR-10-LABX-0039). We acknowledge support by Universidad de Buenos Aires (UBACyT No.20020130100570BA) and the LIA PMF-FMF (Franco-Argentinian International Associated Laboratory in the Physics and Mechanics of Fluids). GLM acknowledges support by Universidad Nacional de Entre Ríos (PID-SCYT-UNER N˚ 6173-2017).

Conflicts of Interest

The authors declare no conflict of interest.

References

[1] Haig, S.J., Collins, G., Davies, R.L., Dorea, C.C. and Quince, C. (2011) Biological Aspects of Slow sand Filtration: Past, Present and Future. *Water Science & Technology Water Supply*, **11**, 468-472. https://doi.org/10.2166/ws.2011.076

[2] Rippy, A.M. (2015) Meeting the Criteria: Linking Biofilter Design to Fecal Indicator Bacteria Removal. *WIREs Water*, **2**, 577-592. https://doi.org/10.1002/wat2.1096

[3] Verma, S., Daverey, A. and Sharma, A. (2017) Slow Sand Filtration for Water and Wastewater Treatment—A Review. *Environmental Technology Review*, **6**, 47-58. https://doi.org/10.1080/21622515.2016.1278278

[4] Ginn, T.R., Wood, B.D., Nelson, K.E., Scheibe, T.D., Murphy, E.M. and Clement, T.P. (2002) Processes in Microbial Transport in the Natural Subsurface. *Advances in Water Resources*, **25**, 1017-1042. https://doi.org/10.1016/S0309-1708(02)00046-5

[5] Stevik, T.K., Aa, K., Ausland, G. and Hanssen, J.F. (2004) Removal of Pathogenic Bacteria in Wastewater Percolating through Porous Media: A Review. *Water Research*, **38**, 1355-1367. https://doi.org/10.1016/j.watres.2003.12.024

[6] Nelson, K.E., Massoudieh, A. and Ginn, T.R. (2007) *E. coli* Fate and Transport in

the Happel Sphere-in-Cell Model. *Advances in Water Resources*, **30**, 1492-1504. https://doi.org/10.1016/j.advwatres.2006.05.027

[7] Hill, J., Kalkanci, O., McMurry, J.L. and Koser, H. (2007) Hydrodynamic Surface Interactions Enable *Escherichia coli* to Seek Efficient Routes to Swim Upstream. *Physical Review Letters*, **98**, Article ID: 068101. https://doi.org/10.1103/PhysRevLett.98.068101

[8] Marcos, Fu, H.C., Powers, T.R. and Stocker, R. (2012) Bacterial Rheotaxis. *Proceedings of the National Academy of Sciences of the United States of America*, **109**, 4780-4785. https://doi.org/10.1073/pnas.1120955109

[9] Altshuler, E., Miño, G., Pérez-Penichet, C., del Río, L., Lindner, A., Rousselet, A. and Clément, E. (2013) Flow-Controlled Densification and Anomalous Dispersion of *E. coli* through a Constriction. *Soft Matter*, **9**, 1864-1870. https://doi.org/10.1039/C2SM26460A

[10] Rusconi, R., Guasto, J.S. and Stocker, R. (2014) Bacterial Transport Suppressed by Fluid Shear. *Nature Physics*, **10**, 212-217. https://doi.org/10.1038/nphys2883

[11] Figueroa-Morales, N., Miño, G.L., Rivera, A., Caballero, R., Clement, E., Altshuler, E. and Lindner, A. (2015) Living on the Edge: Transfer and Traffic of *E. coli* in a Confined Flow. *Soft Matter*, **11**, 6284-6293. https://doi.org/10.1039/C5SM00939A

[12] Archer, C.T., Kim, J.F., Jeong, H., Park, J.H., Vickers, C.E., Lee, S.Y. and Nielsen, L.K. (2011) The Genome Sequence of *E. coli* W (ATCC 9637): Comparative Genome Analysis and an Improved Genome-Scale Reconstruction of *E. coli*. *BMC Genomics*, **12**, 1-20. https://doi.org/10.1186/1471-2164-12-9

[13] Prüss, B.M. and Matsumura, P. (1997) Cell Cycle Regulation of Flagellar Genes. *Journal of Bacteriology*, **179**, 5602-5604. https://doi.org/10.1128/jb.179.17.5602-5604.1997

[14] Minamino, T., Imae, Y., Oosawa, F., Kobayashi, Y. and Oosawa, K. (2003) Effect of Intracellular pH on Rotational Speed of Bacterial Flagellar Motors. *Journal of Bacteriology*, **185**, 1190-1194. https://doi.org/10.1128/JB.185.4.1190-1194.2003

[15] Tinevez, J.-Y., Perry, N., Schindelin, J., Hoopes, G.M., Reynolds, G.D., Laplantine, E., Bednarek, S.Y., Shorte, S.L. and Eliceiri, K.W. (2017) TrackMate: An Open and Extensible Platform for Single-Particle Tracking. *Methods*, **115**, 80-90. https://doi.org/10.1016/j.ymeth.2016.09.016

[16] Lauga, E., DiLuzio, W.R., Whitesides, G.M. and Stone, H.A. (2006) Swimming in Circles: Motion of Bacteria near Solid Boundaries. *Biophysical Journal*, **90**, 400-412. https://doi.org/10.1529/biophysj.105.069401

[17] Li, G., Bensson, J., Nisimova, L., Munger, D., Mahautmr, P., Tang, J.X., Maxey, M.R. and Brun, Y.V. (2011) Accumulation of Swimming Bacteria near a Solid Surface. *Physical Review E*, **84**, Article ID: 041932. https://doi.org/10.1103/PhysRevE.84.041932

[18] Guidobaldi, H.A., Jeyaram, Y., Condat, C.A., Oviedo, M., Berdakin, I., Moshchalkov, V.V., Giojalas, L.C., Silhanek, A.V. and Marconi, V.I. (2015) Disrupting the Wall Accumulation of Human Sperm Cells by Artificial Corrugation. *Biomicrofluidics*, **9**, Article ID: 024122. https://doi.org/10.1063/1.4918979

[19] Leptos, K.C., Guasto, J.S., Gollub, J.P., Pesci, A.I. and Goldstein, R.E. (2009) Dynamics of Enhanced Tracer Diffusion in Suspensions of Swimming Eukaryotic Microorganisms. *Physical Review Letters*, **103**, Article ID: 198103. https://doi.org/10.1103/PhysRevLett.103.198103

[20] Miño, G., Mallouk, T.E., Darnige, T., Hoyos, M., Dauchet, J., Dunstan, J., Soto, R.,

Wang, Y., Rousselet, A. and Clemént, E. (2011) Enhanced Diffusion Due to Active Swimmers at a Solid Surface. *Physical Review Letters*, **106**, Article ID: 048102.

[21] Jeffery, G.B. (1922) The Motion of Ellipsoidal Particles Immersed in a Viscous Fluid. *Proceedings of the Royal Society of London. Series A*, **102**, 161-179. https://doi.org/10.1098/rspa.1922.0078

[22] DiLuzio, W.R., Turner, L., Mayer, M., Garstecki, P., Weibel, D.B., Berg, H.C. and Whitesides, G.M. (2005) Escherichia Coli Swim on the Right-Hand Side. *Nature*, **435**, 1271-1274. https://doi.org/10.1038/nature03660

[23] Sartori, P., Chiarello, E., Jayaswal, G., Pierno, M., Mistura, G., Brun, P., Tiribocchi, A. and Orlandini, E. (2018) Wall Accumulation of Bacteria with Different Motility Patterns. *Physical Review E*, **97**, Article ID: 022610. https://doi.org/10.1103/PhysRevE.97.022610

[24] Takagi, D., Palacci, J., Braunschweig, A.B., Shelley, M.J. and Zhang, J. (2014) Hydrodynamic Capture of Microswcimmers into Sphere-Bound Orbits. *Soft Matter*, **10**, 1784-1789. https://doi.org/10.1039/c3sm52815d

[25] Sipos, O., Nagy, K., Di Leonardo, R. and Galajda, P. (2015) Hydrodynamic Trapping of Swimming Bacteria by Convex Walls. *Physical Review Letters*, **114**, Article ID: 258104. https://doi.org/10.1103/PhysRevLett.114.258104

Supplementary Material

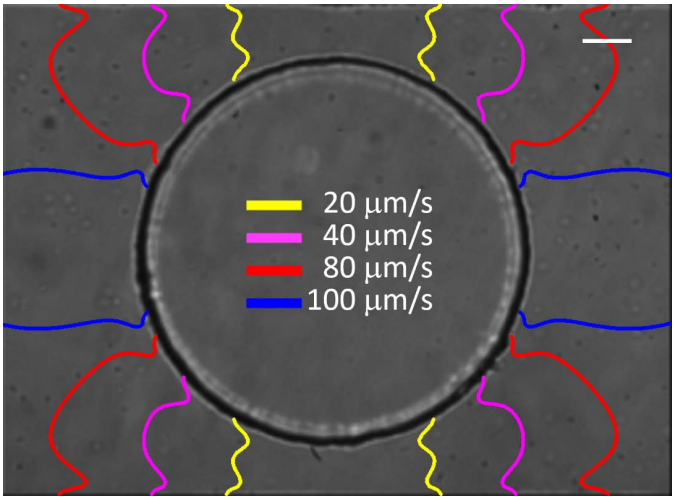

Figure S1. Superposition of curves at same mean shear rates $<\dot{\gamma}> = 5s^{-1}$ obtained from the simulation at different flows U (yellow, U = 20 µm/s; magenta, U = 40 µm/s; green, red, U = 70 µm/s; and blue, U = 100 µm/s). Top-left bar = 20 µm.

Supplementary_Movie_SM1 and Supplementary_Movie_SM1_tracks show an example of bacterial suspension flowing at U = 55 µm/s and the interaction with the obstacle. The second movie exemplifies the tracks obtained with Track Mate. Scale bar represents 20 µm.

Supplementary_Movie_SM1

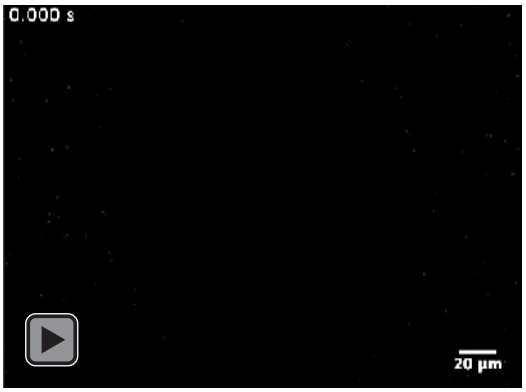

Supplementary_Movie_SM1_Tracks